Dynamical symmetry breaking of U(N)-symmetric gauge theory in the $1/N$ expansion*

J. S. Kang
Department of Physics, Brandeis University, Waltham, Massachusetts 02154
(Received 29 April 1976)

A gauge theory with U(N) symmetry is studied in the large-N limit to all orders in the scalar self-coupling, and to lowest nontrivial order in the gauge coupling. Unlike the $1/N$ expansion of the scalar field theory, the effective potential is found to be always real, although it can be mutiple-valued. Furthermore, there is a region in the coupling-constant space where symmetry is broken spontaneously involving two separate phase transitions, one of the first kind and one of the second kind. This phenomenon persists for arbitrarily small (finite) gauge coupling as a genuine feature of the $1/N$ expansion, exhibiting much more of the nonlinear structure of the complete theory than found in ordinary perturbation expansions. A comparison is made between the spontaneous symmetry breaking found in the $1/N$ expansion and that of other symmetry-breaking schemes, which are of the Goldstone, Higgs, or Coleman-Weinberg type. Here the vector-scalar-boson mass ratio, m_V^2/m_S^2, is of $O(g^2)$, which is contrasted with Higgs and Coleman-Weinberg mechanisms, for which m_V^2/m_S^2 is of $O(1)$ and $O(g^{-2})$, respectively, where g is the gauge coupling.

I. INTRODUCTION

Recently the many-field limit of quantum field theories has attracted considerable attention as part of the continuing attempt to understand the underlying physical content of such theories in a way which does not depend on the ordinary perturbation expansion in the coupling constants.[1] A typical model is a field theory with an internal symmetry O(N) or U(N), with N chosen as the new expansion parameter. Then the coupling constants need not be small, and the $1/N$ expansion contains much more nonlinear structure of the exact theory than the ordinary loop expansion. It has an infinite number of Feynman diagrams even in leading-order approximation. The new expansion has some application to the strong-interaction theory, since it has been shown that a gauge theory with U(N) color symmetry is described by the planar diagrams in the large-N limit, which is topologically equivalent to the dual resonance models.[2] It may also be relevant to unified gauge groups of weak interactions if these groups become sufficiently large.

In four-dimensional space-time most of the previous work has concentrated on the O(N)-symmetric $\lambda\phi^4$ theory. Initial studies of this model incorrectly indicated that the $1/N$ expansion was not consistent, claiming that the Green's functions generate tachyons[3] and that the next-to-leading term destabilized the vacuum state by making the effective potential everywhere complex.[4] However, a careful reanalysis has shown that the effective potential $V(\phi^2)$ is in fact a double-valued real function of ϕ^2, with its absolute minimum always lying in the second real solution of the gap equation, features which were previously overlooked.[5] Then the $1/N$ expansion of O(N)-symmetric $\lambda\phi^4$ theory becomes a consistent theory if the Green's functions are constructed with respect to the global minimum of $V(\phi^2)$. Tachyons disappear and the $1/N$ correction to $V(\phi^2)$ is still stable at the true ground state.[5] Further, spontaneous symmetry breakdown is not possible and there exist a bound state and a resonance in the strong-coupling domain.[5]

The purpose of this paper is to add gauge fields to this theory. We consider a U(N)-symmetric gauge theory in the large-N limit. The composite field χ is introduced as in the scalar model,[3,6] and the topologies of the diagrams are studied to leading approximation in N. It is shown that only *certain* planar diagrams are dominant in the large-N limit. We find it very complicated to evaluate the effective potential even to leading order in N. Therefore, we confine ourselves to $V(\phi^2)$ computed to lowest nontrivial order in the gauge coupling, but to all orders in the scalar self-coupling constant. Our result cannot be reliable if the gauge coupling g^2 is too large. Nevertheless, we find that new and interesting phenomena occur even in the weak gauge coupling region. The effective potential is now a triple-valued function of ϕ^2 in general and it is everywhere real. Furthermore, there is a region in the coupling-constant space where symmetry breakdown can occur. These results can be contrasted with other symmetry-breaking schemes such as the Higgs[7] and the Coleman-Weinberg mechanisms,[8] which are usually discussed in the context of an ordinary perturbation expansion in small coupling constants. Our effective potential has three real solutions in general; we show that one of them reduces to $V(\phi^2)$ of ordinary perturbation theory in the weak-coupling limit, and symmetry breakdown of the Higgs or the Coleman-Weinberg type can be attributed to the local minimum of $V(\phi^2)$ occurring on this particular solution. However, the *global* minimum occurs on one of the other real solutions of the effective potential in our shceme, owing to the rich nonlinear structure of the $1/N$ expansion, and it breaks the symmetry of the theory *spontaneously*. We also note that the vector-scalar mass ratio is of $O(g^2)$ here, while it is of $O(1)$ in the Higgs scheme and $O(1/g^2)$ in the Coleman-Weinberg scheme, where g is the gauge coupling constant.

The plan of this paper is as follows: In Sec. II we review U(N)-symmetric $\lambda\phi^4$ theory as a preliminary to the extension of the gauge theory. No new result is presented in this section, but some technical points are emphasized here. Here we choose U(N) symmetry instead of O(N), use the dimensional regularization method instead of the ordinary cutoff method, and utilize Eq. (2.13) maximally for the study of the effective potential without solving the transcendental gap equation (2.11) explicitly. In Sec. III we discuss a U(N)-symmetric gauge theory with one scalar multiplet. First we study the class of Feynman diagrams which are dominant in the large-N limit. Then we construct the effective potential to lowest nontrivial order in g^2, renormalize $V(\phi^2)$, and analyze the result. It is shown that there are four kinds of phases depending upon the values of the coupling constants, and there is a region in the λ-g^2 plane for which symmetry is spontaneously broken. Typical behavior of the effective potential as well as the particle masses are studied as a function of g^2. In Sec. IV we compare a new symmetry-breaking scheme to other well-known mechanisms of the Higgs type or the Coleman-Weinberg type.

II. THE $1/N$ EXPANSION OF U(N)-SYMMETRIC $\lambda\phi^4$ THEORY

This section contains essentially nothing new other than the results which have been found in the $1/N$ expansion of O(N)-symmetric $\lambda\phi^4$ theory.[1,3,5] Nevertheless, we shall discuss a scalar theory with U(N) symmetry here as a preliminary to the study of the $1/N$ expansion in gauge theories. We intend this section to be self-contained, but shall be as brief as possible, since O(N)-symmetric scalar theory has been extensively investigated in the literature.[1,3,4,5]

Let us consider a scalar field theory with the scalar field belonging to the vector representation of U(N). Then the Lagrangian of the theory becomes

$$N^{-1}\mathcal{L} = (\partial_\mu \phi_0^*)(\partial^\mu \phi_0) - \mu_0^2\phi_0^*\phi_0 - \tfrac{1}{2}\lambda_0(\phi_0^*\phi_0)^2\,, \tag{2.1}$$

where ϕ_0 is an N-component complex scalar field and the subscript 0 refers to the bare quantities. An overall factor N is introduced in the Lagrangian, which leads to exactly the same results presented in the existing literature.[1,3,5] It only simplifies the discussion of the dominant Feynman diagrams in any given order of the $1/N$ expansion.

Owing to the additional factor N in our Lagrangian, every vertex in a Feynman diagram is of $O(N)$ while every internal propagator is of $O(1/N)$. This is reminiscent of the loop expansion, where one expands the theory in terms of the Planck constant $\hbar$.[9] However, there is an important difference between the two expansions, one in $1/N$ and the other in $\hbar$. Since the scalar loops *can* add additional powers in N, the $1/N$ expansion contains many more diagrams in every order than the ordinary loop expansion. In fact, there are an infinite number of Feynman diagrams even in leading order.[1] It is this rich structure of the $1/N$ expansion that enables us to study a strong-coupling theory.

The effective potential for the Lagrangian, given in Eq. (2.1), can be most conveniently calculated by the introduction of a composite field χ,[3]

$$\begin{aligned}N^{-1}\mathcal{L} &= (\partial_\mu \phi_0^*)(\partial^\mu \phi_0) - \mu_0^2\phi_0^*\phi_0 - \tfrac{1}{2}\lambda_0(\phi_0^*\phi_0)^2 \\ &\quad + \frac{1}{2\lambda_0}(\chi_0 - \mu_0^2 - \lambda_0\phi_0^*\phi_0)^2 \\ &= (\partial_\mu \phi_0^*)(\partial^\mu \phi_0) + \frac{1}{2\lambda_0}\chi_0^2 - \frac{\mu_0^2}{\lambda_0}\chi_0 - \chi_0\phi_0^*\phi_0\,.\end{aligned} \tag{2.2}$$

Then the effective potential $V(\phi^2)$ to leading order in the $1/N$ expansion becomes

$$N^{-1}V(\phi^2) = -\frac{1}{2\lambda_0}\chi_0^2 + \frac{\mu_0^2}{\lambda_0}\chi_0 + \chi_0\phi_0^*\phi_0 + \int\frac{d^4k}{(2\pi)^4}\ln(k^2+\chi_0)\,, \tag{2.3}$$

where $\phi = (\phi^*\phi)^{1/2}$ and the integration is to be carried out in Euclidean space. Furthermore, we should eliminate the χ field by means of the "gap equation"

$$\frac{\partial V}{\partial \chi_0} = 0\,, \tag{2.4}$$

i.e.,

$$\frac{1}{\lambda_0}\chi_0(\phi_0^2) = \frac{\mu_0^2}{\lambda_0} + \phi_0^2 + \int\frac{d^4k}{(2\pi)^4}\frac{1}{k^2+\chi_0(\phi_0^2)}\,. \tag{2.5}$$

The effective potential in Eq. (2.3) contains infinities which are very familiar in quantum field theories, with renormalization necessary before one can analyze the ground state of our theory. We shall choose *the renormalization point at $\phi^2 = 0$ which is on the orbit defined by Eq. (2.4)* and impose the following renormalization condition:

$$N^{-1}\frac{dV}{d\phi^2}\bigg|_{\phi^2=0}=\chi(0)=\mu^2, \tag{2.6}$$

$$N^{-1}\frac{d^2V}{d\phi^4}\bigg|_{\phi^2=0}=\lambda. \tag{2.7}$$

For the moment we shall assume that μ^2 is positive, but λ can have any sign. Later we shall also discuss the case of negative μ^2.

It is well known that there is no wave-function renormalization to leading order in the $1/N$ expansion in the scalar field theory. This means that the composite field χ_0 does not need wave-function renormalization either, since the χ-ϕ^*-ϕ three-point vertex does not have any divergent diagrams in this order. Therefore, we only need a mass renormalization and a coupling-constant renormalization. Since we plan to extend the present theory to non-Abelian gauge theory in the next section, we shall adopt, dimensional regularization, which is a gauge-invariant regularization method.[10] Then from Eqs. (2.3)–(2.7) we find the relations between the renormalized and the bare quantities

$$\frac{1}{\lambda}=\frac{1}{\lambda_0}+\frac{1}{16\pi^2}\frac{1}{\epsilon}, \tag{2.8}$$

$$\frac{\mu^2}{\lambda}=\frac{\mu_0{}^2}{\lambda_0}-\frac{\mu^2}{16\pi^2}, \tag{2.9}$$

where the integration is performed in $(4-2\epsilon)$-dimensional Euclidean space. Finally we obtain the renormalized effective potential

$$N^{-1}V=-\frac{1}{2\lambda}\chi^2+\frac{\mu^2}{\lambda}\chi+\chi\phi^2+\frac{1}{32\pi^2}\left[\chi^2\left(\ln\frac{\chi}{\mu^2}-\frac{3}{2}\right)+2\mu^2\chi\right]. \tag{2.10}$$

Now let us analyze Eq. (2.10). The gap equation (2.4) defines the orbit for λ in the form of a transcendental function in ϕ^2,

$$\phi^2=-\frac{\mu^2}{\lambda}+\frac{1}{\lambda}\chi-\frac{1}{16\pi^2}\left[\chi\left(\ln\frac{\chi}{\mu^2}-1\right)+\mu^2\right], \tag{2.11}$$

or

$$\Phi^2\equiv\phi^2+\frac{\mu^2}{\lambda}+\frac{\mu^2}{16\pi^2}=\chi\left(\frac{1}{\lambda}+\frac{1}{16\pi^2}-\frac{1}{16\pi^2}\ln\frac{\chi}{\mu^2}\right). \tag{2.12}$$

We show this orbit in Fig. 1. Since the Euclidean integral in Eq. (2.5) is real for real positive χ, only the principal Riemann sheet of Eq. (2.12) is to be considered. We also note from Eq. (2.10) that

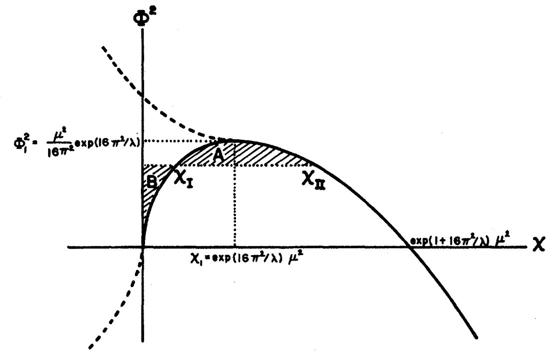

FIG. 1. Typical behavior of the orbit in U(N) $\lambda\phi^4$ theory. When $\Phi^2>\Phi_1{}^2$ or $\Phi^2<0$, χ becomes complex and only its real part is plotted, shown as dotted lines.

$$N^{-1}\frac{dV}{d\Phi^2}=N^{-1}\frac{\partial V}{\partial\Phi^2}+N^{-1}\frac{\partial V}{\partial\chi}\frac{d\chi}{d\Phi^2}=\chi. \tag{2.13}$$

Therefore, the value of the composite field χ on the orbit is the same as the slope of the effective potential, and $V(\phi^2)$ can be obtained by quadratures in the χ-Φ^2 plane. This is very important in our analysis, since we are able to deduce the behavior of the effective potential as a function of Φ^2 without solving the transcendental equation (2.12) explicitly. It is clear from Fig. 1 that there are in general two solutions for χ for any given value of Φ^2, and accordingly $V(\Phi^2)$ becomes a double-valued function of Φ^2. We shall divide the orbit into two parts, solution I and solution II, as shown in Fig. 1. Then the effective potential with solution I, $V_{\rm I}(\Phi^2)$, is simply area B in Fig. 1. To get $V_{\rm II}(\Phi^2)$ we should integrate the orbit up to $\Phi_1{}^2$ and come back to Φ^2, which means that

$$V_{\rm I}(\Phi^2)=B, \qquad V_{\rm II}(\Phi^2)=B-A. \tag{2.14}$$

Equation (2.14) tells us immediately that the effective potential is always lower on solution II than on solution I. We have plotted $V(\Phi^2)$ in Fig. 2. Since there is no real solution of the gap equation for $\Phi^2>\Phi_1{}^2$, χ becomes complex in this region, and thus $V(\Phi^2)$ becomes also complex for $\Phi^2>\Phi_1{}^2$. The same is true of $V_{\rm I}(\Phi^2)$ for $\Phi^2<0$.

The ground state of the theory is the absolute minimum of $V(\Phi^2)$ for $\phi^2>0$. Therefore, only part of the effective potential in Fig. 2 should be taken into account, i.e.,

$$\Phi^2>\Phi_0{}^2\equiv\left(\frac{1}{\lambda}+\frac{1}{16\pi^2}\right)\mu^2. \tag{2.15}$$

It is trivial to prove that $\Phi_0{}^2\leq\Phi_1{}^2$ always, which

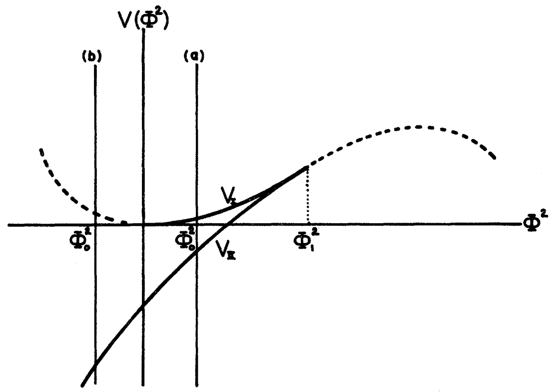

FIG. 2. Typical behavior of the effective potential in the $\lambda\phi^4$ theory. When $V(\phi^2)$ becomes complex, only its real part is plotted, shown as dotted lines. Since $V(\phi^2)$ is shown as a function of Φ^2, only that part of $V(\phi^2)$ for which $\Phi^2 > \Phi_0{}^2$ is to be considered for the analysis of the ground state.

leaves the following cases:

(*a*) $0 \leqslant \Phi_0{}^2 \leqslant \Phi_1{}^2$. In this case there are two local minima, one on each solution. Both minima are U(N)-symmetric.

(*b*) $\Phi_0{}^2 < 0$. We also have two local minima in this case. However, the minimum of $V_{\rm I}(\phi^2)$ breaks U(N) symmetry while the one on solution II is still U(N)-symmetric.

Now we shall study the Green's functions in order to verify which of the candidates corresponds to the true ground state of our theory. To leading order in N, there is only one diagram to be calculated for the two-point Green's functions (Fig. 3). Therefore, we have

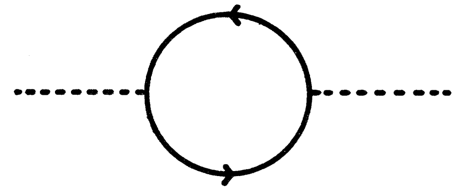

FIG. 3. A diagram which contributes to the Green's function (2.16). The dotted line refers to the χ field, and the solid index line with direction refers to the scalar field.

$$G^{-1}(p^2) = iN \begin{pmatrix} -1/\lambda_0 - B(\chi;p^2) & \phi^j \\ \phi_i & (p^2+\chi)\delta_i^j \end{pmatrix}, \tag{2.16}$$

where

$$B(\chi;p^2) = \int \frac{d^4k}{(2\pi)^4} \frac{1}{k^2+\chi} \frac{1}{(k+p)^2+\chi}, \tag{2.17}$$

and a Wick rotation is made so that all the momenta k and p are in Euclidean space. It is straightforward to invert (2.16), giving

$$G(p^2) = -\frac{i}{N} \begin{pmatrix} -\dfrac{p^2+\chi}{D(\chi,\phi^2;p^2)} & \dfrac{\phi^j}{D(\chi,\phi^2;p^2)} \\ \dfrac{\phi_i}{D(\chi,\phi^2;p^2)} & \dfrac{1}{p^2+\chi}\left(\delta_i^j - \dfrac{\phi_i\phi^j}{\phi^2}\right) + \dfrac{1/\lambda_0 + B(\chi;p^2)}{D(\chi,\phi^2;p^2)} \dfrac{\phi_i\phi^j}{\phi^2} \end{pmatrix}, \tag{2.18}$$

where

$$D(\chi,\phi^2;p^2) = (p^2+\chi)\left[\frac{1}{\lambda_0} + B(\chi;p^2)\right] + \phi^2. \tag{2.19}$$

Of course $B(\chi;p^2)$ as it stands in Eq. (2.17) is divergent, but it is made finite by the coupling-constant renormalization. When $B(\chi;p^2)$ is calculated in $(4-2\epsilon)$-dimensional space and Eq. (2.8) is taken into account, we find a finite expression for $D(\chi,\phi^2;p^2)$,

$$D(\chi,\phi^2;p^2) = (p^2+\chi)\left\{\frac{1}{\lambda} - \frac{1}{16\pi^2}\ln\frac{\chi}{\mu^2} + \frac{1}{8\pi^2}\left[1 - \left(\frac{p^2+4\chi}{p^2}\right)^{1/2} \ln\frac{(p^2+4\chi)^{1/2}+\sqrt{p^2}}{2\sqrt{\chi}}\right]\right\} + \phi^2. \tag{2.20}$$

Since the $D(\chi,\phi^2;p^2)$'s appear as denominators in the Green's function (2.18), the zeros of $D(\chi,\phi^2;p^2)$ correspond to particle masses. However, to avoid the tachyon problem, it is important for Eq. (2.20) not to have any zeros between $p^2=0$ and $p^2=+\infty$ (recall that p^2 is Euclidean).

Going back to the various candidates for the ground state, we shall consider an asymmetric vacuum first, which can be realized when $\Phi_0{}^2<0$ [the minimum of $V_{\rm I}$ in case (b) of Fig. 2]. Then we have

$$\chi = 0, \quad \phi^2 \neq 0, \tag{2.21}$$

and

$$D(0,\phi^2;p^2) = p^2\left[\frac{1}{\lambda} + \frac{1}{16\pi^2}\left(2 - \ln\frac{p^2}{\mu^2}\right)\right] + \phi^2. \tag{2.22}$$

Since $D(0, \phi^2; 0) = \phi^2$ and $D(0, \phi^2; \infty) = -\infty$, we learn immediately that an asymmetric vacuum always has tachyons, and must be ruled out. The second possibility is a symmetric vacuum,

$$\chi \neq 0, \quad \phi^2 = 0, \tag{2.23}$$

and Eq. (2.20) becomes

$$D(\chi, 0; p^2) = (p^2+\chi)\left\{\frac{1}{\lambda} - \frac{1}{16\pi^2}\ln\frac{\chi}{\mu^2} + \frac{1}{8\pi^2}\left[1 - \left(\frac{p^2+4\chi}{p^2}\right)^{1/2}\ln\frac{(p^2+4\chi)^{1/2}+\sqrt{p^2}}{2\sqrt{\chi}}\right]\right\}. \tag{2.24}$$

It can be readily seen that the expression inside the square brackets is a monotonically decreasing function in p^2, which goes to $-\infty$ asymptotically. Therefore, the necessary and sufficient condition for the absence of tachyons is that the expression inside the curly brackets should be negative at $p^2 = 0$, i.e.,

$$\frac{\chi}{\mu^2} > \exp\left(\frac{16\pi^2}{\lambda}\right). \tag{2.25}$$

This inequality is always satisfied on solution II, which is clearly shown in Fig. 1. Thus the true ground state of the theory should be the U(N)-symmetric vacuum of $V_{II}(\phi^2)$.[5] Therefore, we have learned a lesson from the analysis of $V(\phi^2)$: *The theory becomes a consistent one if the global minimum of the effective potential is chosen for the ground state.* This is further evidenced by a study of the higher-order correction in N. The next-to-leading term is always complex on solution I,[4] while there exists a finite region containing the symmetric vacuum of solution II, for which the $1/N$ correction term remains real.[5]

Before we discuss the case for $\mu^2 < 0$, a remark is in order about the renormalization conditions (2.6) and (2.7). Although we have chosen $\phi^2 = 0$ (or $\Phi^2 = \Phi_0^2$) as our renormalization point, there could be an ambiguity in this prescription owing to the double-valued nature of the effective potential. In this event at least one of the solutions should satisfy the renormalization conditions. Recalling that Eqs. (2.6) and (2.7) define the slope and the curvature of $V(\Phi^2)$ respectively at $\Phi^2 = \Phi_0^2$, we notice immediately that the renormalization point is on solution I for $\lambda > 0$ while it lies on solution II for $\lambda < 0$. This illustrates the fact that two sets of the renormalization conditions give rise to the identical effective potential.

We must be more careful when $\mu^2 < 0$. According to Eq. (2.5), we have an inconsistency appearing if $\chi(0)$ is real and negative. Therefore, the effective potential becomes complex near the renormalization point $\phi^2 = 0$, and Eqs. (2.6) and (2.7) should be regarded to hold for the $\mathrm{Re}V(\phi^2)$ only. This is quite legitimate since the divergences in Eq. (2.3) are real, and only the real part of the gap equation and V need to be renormalized. However, the renormalization conditions can be replaced by another equivalent set of conditions with $\mu^2 > 0$ and $\lambda < 0$, as can be seen from Fig. 2. This is only possible when the effective potential is double-valued. It is customary in conventional perturbation theory to fix the sign of λ to be positive, but take μ^2 to be of any sign. In other words, the renormalization point is chosen on solution II. However, in the $1/N$ expansion it is most convenient to choose positive μ^2 with any sign for λ.

Even the massless theory can be considered from the effective potential shown in Fig. 2. Since $\chi_I = 0$ at $\Phi_0^2 = 0$, $V_I(\Phi^2 = \phi^2)$ satisfies Eq. (2.6) with $\mu^2 = 0$. However, the same argument does not apply to Eq. (2.7). The renormalized coupling constant becomes infinite at this point, which is due to the infrared divergences in the massless theory. Therefore, the condition (2.7) should be defined at $\phi^2 = M^2 \neq 0$ to avoid the infrared problem. Once again this can be formulated with the equivalent conditions on solution II. Here we simply choose $\lambda = -16\pi^2$ so that Φ_0^2 defined by (2.12) at $\phi^2 = 0$ becomes zero, but vary μ^2 on solution II so that the desired coupling-constant renormalization condition is satisfied on solution I.

We are able to study the strong-coupling theory because our expansion parameter is N^{-1} and not λ. Certain questions naturally arise: What is the relation between the $1/N$ expansion and the conventional perturbation expansion? Is the latter restored in the weak-coupling limit of the $1/N$ expansion? We can answer this question affirmatively in the following way. In the conventional perturbation theory λ is assumed to be *small and positive*. Therefore, we shall choose a renormalization point on solution I and consider the weak-coupling limit. In this limit Φ^2 becomes exponentially infinite, much faster than does Φ_0^2, and the energy difference between the two solutions I and II also becomes infinite. The situation becomes more dramatic in the weak-coupling limit, where conventional perturbation becomes a better approximation. Then we can choose solution I for the description of our theory, and we can ignore solution II. This may sound contradictory considering the tachyon problem that we encountered on solution I. The tachyon mass is independent of N and causes genuine difficulties for the strong-coupling theory on solution I. However, the tachyon mass is a function of λ which becomes infinite in the weak-coupling limit. This is not a reliable result of the theory, for the $1/N$ expansion also fails to be valid in the deep Euclidean region. Therefore, the infinitely heavy tachyon mass in the weak-coupling limit may be an artifact of the theory, and the effective potential on solution I, $V_{\rm I}(\phi^2)$, becomes the effective potential of ordinary perturbation theory. Now the minimum of $V_{\rm I}(\phi^2)$ becomes quasistable and can be chosen as the ground state of the theory. The Goldstone phenomenon[11] can be also realized when $\Phi_0{}^2<0$, but *it is only possible in this theory in the weak-coupling limit.*

It is a folklore of quantum field theory that a negative coupling constant should be excluded from consideration, since the effective potential is then unbounded below. However, results obtained in the $1/N$ expansion cast some doubt on this widespread belief. When λ is negative, $V_{\rm II}$ becomes the effective potential in the perturbation limit. It can be seen in Fig. 2 that $V(\Phi^2)$ becomes complex for large Φ^2 instead of being unbounded below. This illustrates that the higher-order quantum corrections affect the large-Φ^2 behavior and suggests that arguments based on the tree approximation may not be justified in the asymptotic region.

Finally we shall discuss the effective coupling constant. The asymptotic behavior of the coupling constant is normally obtained from the study of $\beta(\lambda)$ in the renormalization-group equation. Since $V(\Phi^2)$ becomes complex for $\Phi^2>\Phi_1{}^2$, $\beta(\lambda(M^2))$ also becomes complex for large M^2, and it is necessary to investigate $\beta(\lambda)$ for complex λ, as has been done by Khuri for simple $\lambda\phi^4$ theory[12] without internal symmetry. However, it is much simpler to calculate the effective coupling constant $\lambda(M^2)$ directly from the effective potential (2.10) as it is the curvature at $\phi^2=M^2$. Since χ is the slope of $V(\Phi^2)$, $\lambda(M^2)$ is the inverse slope of the orbit (2.12), and it can be readily shown that

$$\lambda(M^2)\underset{M^2\to\infty}{\sim}\frac{-1+i}{\ln M^2}. \tag{2.26}$$

Therefore, the effective coupling becomes zero asymptotically, not through the real values, but with the phase angle 135°. Nevertheless this does not necessarily mean that the theory is asymptotically free.[12] Were our expansion parameter the self-coupling constant λ, the vanishing effective coupling would imply that the expansion was a good one in the asymptotic region, and that the theory would be asymptotically free. However, here $1/N$ is our expansion parameter, and the small effective coupling constant does not mean that the leading term of the $1/N$ expansion predicts the correct large-ϕ^2 behavior of the effective potential. It simply means that the next-to-leading terms of the $1/N$ expansion are dominant in the asymptotic limit.

III. A GAUGE THEORY WITH U(N) SYMMETRY

We are now convinced of the consistency of the $1/N$ expansion in the theory, and it is quite natural to extend our study to gauge theories. The non-Abelian gauge theories have attracted a great deal of attention as realistic models for weak and electromagnetic or strong interactions. The $1/N$ expansion of gauge theories may have some particular importance in strong interactions, since it has been shown by 't Hooft that only planar diagrams dominate in the large-N limit of a gauge theory with color gauge group U(N), and thus the topological structure of the $1/N$ expansion is the same as that of the dual models.[2] Therefore, the $1/N$ expansion of a gauge theory with quarks would be a realistic model, but we here shall consider a U(N) gauge theory with scalar quarks in this paper to avoid complications due to the spin of the quarks. Since the vector representation for the scalar field is one of only a few representations which allow the theory to be asymptotically free in the large-N limit,[13] we hope that we do not lose any essential feature of the quark model with a color gauge group. Moreover, our model has the advantage of being presented in four-dimensional space-time, while most of the work with fermion quarks has been restricted to two-dimensional space-time.[2,6]

A. The model

Let us add the U(N) gauge fields $(A_\mu)^i_j$ to the Lagrangian of (2.1), obtaining

$$\begin{aligned}N^{-1}\mathfrak{L} &= (\partial_\mu\phi_0+ig_0A_{0\mu}\phi_0)^*(\partial^\mu\phi_0+ig_0A_0^\mu\phi_0)\\ &\quad-\mu_0{}^2\phi_0^*\phi_0-\tfrac{1}{2}\lambda_0(\phi_0^*\phi_0)^2\\ &\quad-\tfrac{1}{4}\,\mathrm{Tr}\,(F_{\mu\nu}F^{\mu\nu})-\frac{1}{2\xi}\,\mathrm{Tr}\,(\partial_\mu A_0^\mu)^2\\ &\quad-\mathrm{Tr}\,\{\partial_\mu C^*(\partial^\mu C+ig_0[A^\mu,C])\},\end{aligned} \tag{3.1}$$

where

$$F^{\mu\nu}=\partial^\nu A_0^\mu-\partial^\mu A_0^\nu-ig_0[A_0^\mu,A_0^\nu].$$

The scalar field ϕ_0 has N components as in Sec. II, and the gauge field A_μ as well as the ghost field C is an $N\times N$ matrix in the group space. We have chosen U(N) symmetry instead of SU(N) only for technical purposes, but we believe that there is no qualitative change in our final results even if we employ SU(N) for our gauge group. By doing so we have N^2 gauge fields and N^2 ghost fields,[14] so that every element of these $N\times N$ matrices is an independent degree of freedom.

The Feynman rules can be readily derived for the Lagrangian given in (3.1). However, it is most convenient to utilize the group index line in the Feynman rules so that the part of the rules due to the group structure can be considered separately.[2] Then the scalar field carries a single index line whereas the gauge field A and the ghost field C have double lines. It is to be noted that the contravariant indices are not equivalent to the covariant indices unless $N=2$, and thus every index line must be regarded as having a direction. Since every term of the Lagrangian (3.1) is U(N)-invariant, the index lines are always continuous. They are broken neither on the vertices nor on the propagators. Furthermore, the contravariant indices are contracted with the covariant indices, which means that the direction of the line is unchanged along the index line. Therefore, an index line either forms a closed loop, or ends up with an external particle state. In the event an index line closes to form a loop, it gives rise to an additional factor N for the diagram under consideration, since we can assign N indices for the loop. With this simplification of group structure, the remaining part of the Feynman rules can be easily worked out.

Now we introduce the χ field without changing any physics as in Sec. II:

$$\begin{aligned} N^{-1}\mathcal{L} \to N^{-1}\mathcal{L} &+ \frac{1}{2\lambda_0}(\chi_0 - \mu_0{}^2 - \lambda_0\phi_0^*\phi_0)^2 \\ &= (\partial_\mu\phi_0 + ig_0A_{0\mu}\phi_0)^*(\partial^\mu\phi_0 + ig_0A_0^\mu\phi_0) \\ &\quad + \frac{1}{2\lambda_0}\chi_0{}^2 - \frac{\mu_0{}^2}{\lambda_0}\chi_0 - \chi_0\phi_0^*\phi_0 \\ &\quad - \tfrac{1}{4}\,\mathrm{Tr}\,(F_{\mu\nu}F^{\mu\nu}) - \frac{1}{2\xi}\mathrm{Tr}\,(\partial_\mu A_0^\mu)^2 \\ &\quad - \mathrm{Tr}\,\{\partial_\mu C^*(\partial^\mu C + ig_0[A_0^\mu, C])\}\,. \end{aligned} \tag{3.2}$$

The composite field χ is a U(N) singlet, and does not carry any indices. We also note that the four-point self-coupling of the scalar fields is replaced by a trilinear coupling $-\chi\phi^*\phi$, and the mass of the scalar field is generated by the tadpole term, and this trilinear coupling. We shall now study the $1/N$ expansion of the gauge model with the Lagrangian given by (3.2).

B. The $1/N$ expansion of the effective potential

The first step in the calculation of the effective potential is to shift *all* the fields in the Lagrangian (3.2) and to find the effective propagators as well as the effective vertices for the vacuum diagrams.[15] However, we shall shift the χ and ϕ fields only, since the ghost fields do not appear as external particle states and the gauge fields do not develop nonvanishing vacuum expectation values unless the Lorentz symmetry is spontaneously broken. Then the effective Feynman rule shows that the index line can be cut in pieces or part of the line may entirely disappear. Nevertheless this does not contradict what we have discussed earlier. The effective Feynman rule is an *effective* way of replacing the propagators and the vertices with all possible insertions of external fields carrying zero momentum by the effective propagators and the effective vertices, respectively. Therefore, an external scalar field must be attached whenever there is a discontinuity in the index line. It is apparent that a diagram with any index line cut in pieces is at most of the same order in N as the one with such an index line connected, and it becomes of lower order in N if the connected line forms a closed loop. When the index line disappears completely at a certain point, it gives rise to mixed propagators of the χ-ϕ type and ϕ-A type, and induced vertices such as the A_μ-A_μ-ϕ vertices which do not exist in the Lagrangian (3.2).

We are only interested in the leading term of the $1/N$ expansion in this paper and shall now discuss the topology of dominant diagrams in the Landau gauge which we shall choose throughout our work. To do this we have to establish a series of statements as follows.

(1) In the Landau gauge ($\xi=0$) there is no ϕ-A_μ mixed propagator: Suppose that there is such a propagator (Fig. 4) in a Feynman diagram. Then an external ϕ line is to be attached at the disappearance point which gives a vertex proportional to k_μ. However, the vector propagator is transverse in the Landau gauge and becomes zero when contracted with k_μ, i.e.,

$$k_\mu\left(g^{\mu\nu} - \frac{k^\mu k^\nu}{k^2}\right) = 0\,. \tag{3.3}$$

(2) A diagram with χ-ϕ mixed propagators is of lower order in N than the one which is obtained by removing these mixed propagators as well as the χ lines associated with them: Recalling that every vertex is proportional to N, while every propagator is proportional to $1/N$, it is straightforward to

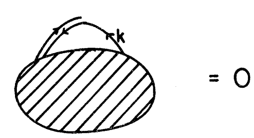

FIG. 4. A schematic illustration of a Feynman diagram with a ϕ-A_μ mixed propagator. The gauge field is denoted by a double line with opposite directions, and the shaded area refers to the rest of the diagram.

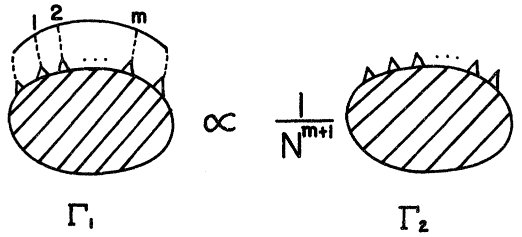

FIG. 5. A schematic illustration of a Feynman diagram with a χ-ϕ mixed propagator.

observe that

$$\Gamma_1 \propto \frac{1}{N^{m+1}} \Gamma_2 \tag{3.4}$$

in Fig. 5 as far as N-power counting is concerned. Since $m \geq 0$ always, a diagram with χ-ϕ mixed propagators cannot be a leading term.

(3) To every diagram with the induced vertices, there corresponds a diagram without them. Furthermore, the two diagrams are of the same order in N: From (1) and (2) we proved that an index line is continuous on the propagators, and thus it can disappear only at the induced vertices. Suppose that a diagram has an induced vertex. Then there should be another induced vertex at the other end of the index line. By connecting them with an index line (a scalar propagator) we removed the induced vertices. The resulting diagram is of the same order as the original one since the factor $1/N$ due to the scalar propagator is to be compensated by the closed-loop factor N.

(4) No internal χ lines are allowed in the leading approximation: By now the dominant diagrams should have their index lines continuous, and thus every line forms a closed loop. We can assume this without loss of generality, for any dominant diagram with the induced vertices can be generated from the above-mentioned prototype diagrams by removing some scalar propagators. Therefore, a diagram Γ_3 with χ lines should have a configuration as in Fig. 6. Then it can be readily shown that

$$\Gamma_3 \propto \frac{1}{N^{m-1}} \Gamma_4 . \tag{3.5}$$

Noting that $m \geq 2$ always (otherwise the diagram is not one-particle-irreducible), we observe that a diagram with internal χ lines cannot be a dominant one. The above statements require that the leading diagrams should satisfy the condition that every index line should be continuous and form a closed loop and no χ propagators are allowed. We have still another statement to describe this class of diagrams.

(5) A diagram of the above-mentioned class is of

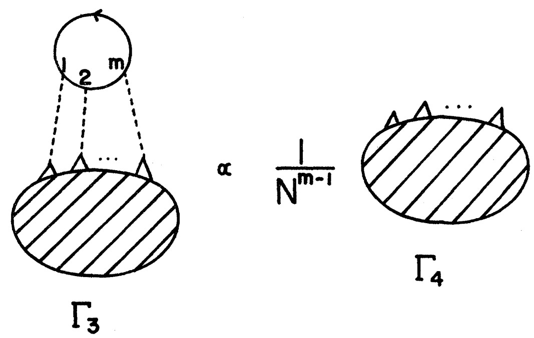

FIG. 6. A schematic illustration of a Feynman diagram with a scalar loop attached to the χ propagator.

order N^{2-2G-S}, where S is the number of scalar loops and G is the genus of the Feynman diagram ($G=0$ for a sphere and $G=1$ for a torus, etc.): Let us assign a fictitious index loop for every scalar loop. Then every internal propagator has double lines and the number of the closed loops, I, is the number of the surfaces bounded by the propagators. If V and P are the number of vertices and propagators of the diagram respectively, then the Euler-Poincaré formula tells us that[16]

$$V - P + I = 2 - 2G , \tag{3.6}$$

where G is the genus of the surface on which the Feynman diagram lies flat. Recalling that a vertex contributes N, a propagator $1/N$, and a closed loop N, and the whole diagram is raised by N^S due to the fictitious index loop, the power of N associated with the diagram is

$$\frac{N^{V-P+I}}{N^S} = N^{2-2G-S} . \tag{3.7}$$

Therefore, the leading diagrams seem to be of $O(N^2)$, which corresponds to $G=0$ and $S=0$. They are planar diagrams with gauge fields and ghost fields only. It turns out that the $O(N^2)$ terms are constants which are independent of χ and ϕ, since the vector fields do not couple to the χ field, and thus the effective potential becomes a constant if we allow all the index lines to form closed loops. We are not interested in additive constants of $V(\phi^2)$ and want to know the next dominant part of this class of diagrams. To obtain a nontrivial contribution to $V(\phi^2)$, we have to cut at least one index line, which reduces the N power by one unit. This means that a diagram which appears to be of $O(N^2)$ is in fact of $O(N)$.

There is another class of diagrams which is of $O(N)$. These diagrams correspond to $G=0$ and $S=1$. Now the diagrams are still planar, but only one scalar loop is allowed. We do not have to break the index lines here since the trilinear coupling $\chi\phi^*\phi$ gives a nontrivial contribution to $V(\phi^2)$.

Therefore, we can conclude that the following class of diagrams is dominant in the large-N limit:

(a) Construct a planar diagram with gauge fields and ghost fields only. Then cut the index line and the closed loop one by one, but on the gauge propagators only, and insert the external fields ϕ.

(b) Construct a planar diagram with only one scalar loop. No index line is to be cut for any insertion.

(c) Remove part of the scalar loop in (b). Then any broken index line due to this process may be further cut for insertion of the external fields ϕ.

C. The effective potential to $O(g^2)$

Although we have found the dominant class of diagrams in the large-N limit, it is nearly impossible to calculate the infinite number of planar diagrams *explicitly*. Therefore, we shall consider the effective potential to leading order in N, but only to $O(g^2)$. Then there are only a few diagrams which need to be calculated. By doing so, we confine ourselves to the study of weak gauge coupling, but the scalar self-coupling constant can be arbitrarily strong.

It can be shown that a diagram with three loops or more is at least of $O(g^4)$. Accordingly, we shall calculate the effective potential up to the two-loop level, but only to leading order in N, and to $O(g^2)$ for the gauge coupling constant. Then the effective potential is the sum of three terms,

$$N^{-1}V(\chi,\phi^2)=N^{-1}V_0+N^{-1}V_1+N^{-1}V_2. \tag{3.8}$$

V_0 is the effective potential in the tree approximation and simply the minus of the nonderivative terms in (3.2) when A_μ and C are set to be zero,

$$N^{-1}V_0=-\frac{1}{2\lambda_0}\chi_0+\frac{\mu_0{}^2}{\lambda_0}\chi_0+\chi_0\phi_0^*\phi_0. \tag{3.9}$$

V_1 is the one loop effective potential and it becomes

$$N^{-1}V_1=\int\frac{d^4k}{(2\pi)^4}\ln\det iD^{-1}(\chi,\phi^2), \tag{3.10}$$

where

$$\det iD^{-1}=\det\begin{vmatrix} -\frac{1}{\lambda} & \phi^j & 0 \\ \phi_i & (k^2+\chi)\delta_i^j & gk^\nu\delta_i^n\phi_m \\ 0 & gk^\mu\delta_k^j\phi^l & (g^{\mu\nu}k^2-k^\mu k^\nu)\delta_k^n\delta_m^l+\frac{1}{\xi}k^\mu k^\nu\delta_k^n\delta_m^l+g^{\mu\nu}g^2(\delta_m^l\phi_k\phi^n+\delta_k^n\phi_m\phi^l)\end{vmatrix}. \tag{3.11}$$

The determinant in (3.11) is to be carried out over the group indices i, j, k, l, m, and n as well as the Lorentz indices μ and ν, and all the quantities λ, ϕ, χ, and g are to be understood as bare ones. We do not have to consider the ghost loop in (3.11) since its contribution to V_1 is a simple constant independent of χ and ϕ^2. It is rather tedious to calculate the giant determinant explicitly, but there is a way of extracting sufficient information for our purposes. After some algebraic manipulation[17] it can be shown that

$$\det iD^{-1}=\det\Delta_1\det\Delta_2\det\Delta_3, \tag{3.12}$$

where

$$\Delta_1=\begin{pmatrix} -\frac{1}{\lambda_0} & \phi^j \\ \phi_i & (k^2+\chi)\delta_i^j\end{pmatrix},$$

$$\Delta_2=[k^2\delta_k^n\delta_m^l+g^2(\delta_m^l\phi^n\phi_k+\delta_k^n\phi^l\phi_m)]^3,$$

$$\Delta_3=\begin{pmatrix} k^2\delta_k^n\delta_m^l+\xi g^2\frac{k^2}{(k^2+\chi)\phi^2}(\phi^2\delta_k^n\phi^l\phi_m-\phi^n\phi_k\phi^l\phi_m) \\ +\xi g^2\frac{k^2}{[(k^2+\chi)+\lambda\phi^2]\phi^2}\phi^n\phi_k\phi^l\phi_m\end{pmatrix}.$$

Now $\xi=0$ in the Landau gauge. Therefore, $\det\Delta_3$ becomes a constant which we are not interested in. Then V_1 consists of two terms, one from $\det\Delta_1$ and the other from $\det\Delta_2$. On dimensional grounds the contribution of $\det\Delta_2$ is proportional to ϕ^4, but ϕ is always combined with the gauge coupling g in Δ_2, which means that Δ_2 is of $O(g^4)$ and does not contribute to V_1 to order $O(g^2)$. Therefore, V_1 takes a surprisingly simple form in our approximation,

$$N^{-1}V_1=\int\frac{d^4k}{(2\pi)^4}\ln(k^2+\chi_0)+O(1/N)+O(g^4). \tag{3.13}$$

There are five two-loop diagrams in the large-N limit, but only two of them are of $O(g^2)$. They are shown in Fig. 7. They can be evaluated straightforwardly[18]:

$$N^{-1}V_{2a}=0, \tag{3.14a}$$

$$N^{-1}V_{2b}=\left(\frac{1}{16\pi^2}\right)^2 g_0{}^2\chi_0{}^2\left[-3\ln^2\frac{\chi_0}{M^2}+\left(\frac{3}{\epsilon}+10\right)\ln\frac{\chi_0}{M^2}+c\right]. \tag{3.14b}$$

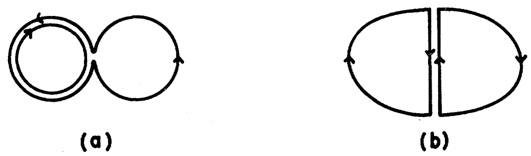

FIG. 7. Two two-loop diagrams which contribute to $V(\phi^2)$ to $O(g^2)$ in the large-N limit. All other two-loop diagrams are either of $O(g^4)$ or of lower order in N.

The loop integrations are carried out in $(4-2\epsilon)$-dimensional Euclidean space, and an arbitrary mass parameter M is introduced.[19] The most convenient choice of M will be given later. The vanishing contribution of the diagram (a) to $O(g^2)$ is due to the "beauty" of dimensional regularization. Since the four-point vertex provides the factor g^2, the vector propagator should remain massless, and the subintegral of the massless propagator becomes zero. The constant c in (3.14b) is not calculated explicitly, but it will be shown later that this constant will be subtracted away in the process of renormalization.

Therefore, we obtain the unrenormalized effective potential to $O(g^2)$ in the large-N limit by adding (3.9), (3.13), and (3.14b),

$$N^{-1}V(\chi,\phi^2) = -\frac{1}{2\lambda_0}\chi_0^2 + \frac{\mu_0^2}{\lambda_0}\chi_0 + \chi_0\phi_0^*\phi_0 + \frac{1}{32\pi^2}\chi_0^2\left[-\frac{1}{\epsilon} + \left(\ln\frac{\chi_0}{M^2} - \frac{3}{2}\right) + \epsilon\left(-\frac{1}{2}\ln^2\frac{\chi_0}{M^2} + \frac{3}{2}\ln\frac{\chi_0}{M^2} - \frac{7}{4}\right)\right] + \left(\frac{1}{16\pi^2}\right)^2 g_0^2\chi_0^2\left[-3\ln^2\frac{\chi_0}{M^2} + \left(\frac{3}{\epsilon}+10\right)\ln\frac{\chi_0}{M^2} + c\right]. \tag{3.15}$$

D. Renormalization

We should renormalize the effective potential given in (3.15) before we analyze it. We shall impose the same renormalization conditions as in Sec. II, i.e.,

$$N^{-1}\frac{dV}{d\phi^2}\bigg|_{\phi^2=0} = \mu^2, \tag{2.6}$$

$$N^{-1}\frac{d^2V}{d\phi^4}\bigg|_{\phi^2=0} = \lambda. \tag{2.7}$$

For the reasons that we mentioned in Sec. II, μ^2 is chosen to be positive, but we shall allow λ to have any sign.

The scalar field ϕ_0 now requires wave-function renormalization, as does χ_0. However, they are related to each other, since the three-point vertex $\chi_0\phi_0^*\phi_0$ does not have any divergent diagrams in our approximation. Therefore, we have,

$$\phi_0 = Z_\phi^{1/2}\phi, \quad \chi_0 = \frac{1}{Z_\phi}\chi. \tag{3.16}$$

From Eq. (2.6) we observe that

$$\chi_0(0) = \frac{1}{Z_\phi}\mu^2, \tag{3.17}$$

which suggests that it is most convenient to choose M^2 as

$$M^2 = \frac{1}{Z_\phi}\mu^2. \tag{3.18}$$

Then the renormalization conditions (2.6) and (2.7) become

$$\frac{\mu_0^2}{\lambda_0 Z_\phi} = \frac{\mu^2}{\lambda} + \frac{1}{16\pi^2}\frac{\mu^2}{Z_\phi^2}(1+\epsilon) + \left(\frac{1}{16\pi^2}\right)^2 g^2\mu^2\left(\frac{6}{\epsilon}+14\right), \tag{3.19}$$

$$\frac{1}{\lambda_0 Z_\phi^2} = \frac{1}{\lambda} - \frac{1}{16\pi^2}\frac{1}{Z_\phi^2}\frac{1}{\epsilon} + \left(\frac{1}{16\pi^2}\right)^2 g^2\left(\frac{9}{\epsilon}+24+2c\right). \tag{3.20}$$

The gauge coupling g_0 does not need any renormalization to $O(g^2)$, and thus is simply the same as g.

The wave-function renormalization is yet to be determined. Unfortunately, this cannot be done from the one-loop approximation, since the external lines carry zero momenta. It should be fixed from the self-consistency of the effective potential. Alternatively it can be also determined explicitly from the one-loop diagrams for the scaler propagator. We find Z_ϕ in either way to be

$$Z_\phi = 1 + \frac{1}{16\pi^2}g^2\left(\frac{3}{\epsilon} - \frac{1}{2}\right). \tag{3.21}$$

Then we obtain the renormalized effective potential by inserting the relations (3.19), (3.20), and (3.21) into Eq. (3.15),

$$N^{-1}V(\chi,\phi^2) = -\frac{1}{2\lambda}\chi^2 + \frac{\mu^2}{\lambda}\chi + \chi\phi^2 + \frac{1}{16\pi^2}\,\frac{1}{2}\left[\chi^2\left(\ln\frac{\chi}{\mu^2} - \frac{3}{2}\right) + 2\chi\mu^2\right] + \left(\frac{1}{16\pi^2}\right)^2 \frac{3}{2}g^2\left[\chi^2\left(-\ln^2\frac{\chi}{\mu^2} + 4\ln\frac{\chi}{\mu^2} - 5\right) + 6\chi\mu^2\right]. \tag{3.22}$$

E. Ground state

Now we shall analyze the effective potential (3.22) and look for the absolute minimum of $V(\phi^2)$. Although this is more complicated than its counterpart in the $\lambda\phi^4$ theory, Eq. (2.10), an essential relation in the previous analysis is still applicable to the gauge theory, which is Eq. (2.13),

$$N^{-1}\frac{dV}{d\phi^2}=\chi\,. \tag{2.13}$$

Once again the effective potential can be obtained by quadratures in the χ-ϕ^2 plane, and it is important to study the χ-ϕ orbit carefully. Since the orbit is to be calculated from (2.4), we have

$$\Phi^2\equiv\phi^2+\Phi_0^{\,2}=\chi\left\{\frac{1}{\lambda}+\frac{1}{16\pi^2}+\left(\frac{3g}{16\pi^2}\right)^2-\left[\frac{1}{16\pi^2}+\left(\frac{3g}{16\pi^2}\right)^2\right]\ln\frac{\chi}{\mu^2}+3\left(\frac{g}{16\pi^2}\right)^2\ln^2\frac{\chi}{\mu^2}\right\}, \tag{3.23}$$

where

$$\Phi_0^{\,2}=\left[\frac{1}{\lambda}+\frac{1}{16\pi^2}+\left(\frac{3g}{16\pi^2}\right)^2\right]\mu^2.$$

Let us study the gap equation (3.23) in further detail, for its shape is crucial for our analysis. The slope of the orbit (3.23) becomes

$$\frac{d\phi^2}{d\chi}=\frac{1}{\lambda}-\left[\frac{1}{16\pi^2}+3\left(\frac{g}{16\pi^2}\right)^2\right]\ln\frac{\chi}{\mu^2}+3\left(\frac{g}{16\pi^2}\right)^2\ln^2\frac{\chi}{\mu^2}, \tag{3.24}$$

which is quadratic in $\ln(\chi/\mu^2)$. Thus the slope of the orbit is always positive if

$$0<\lambda<\frac{12g^2}{(1+3g^2/16\pi^2)^2}\,. \tag{3.25}$$

Then the orbit and the effective potential are both monotonically increasing functions of Φ^2. This is illustrated in Fig. 8. We shall define this situation to be phase I.

If the condition (3.25) is not met, the slope of the orbit becomes negative for a certain range of χ, and the orbit takes one of the forms shown in Figs. 9(a), 10(a), and 11(a). It is to be noted that there are three solutions of χ in general for a given Φ^2, and the effective potential becomes a triple-valued function now. Accordingly, the orbit as well as the effective potential has three pieces as shown in Figs. 9, 10, and 11. The values of χ_1 and χ_2 which give Φ^2 local extrema can be readily obtained from Eq. (3.24),

$$\chi_1=\exp\left\{\frac{1}{2}+\frac{16\pi^2}{6g^2}-\frac{1}{2}\left[\left(1+\frac{16\pi^2}{3g^2}\right)^2-\frac{64\pi^2}{\lambda}\frac{16\pi^2}{3g^2}\right]^{1/2}\right\}\mu^2,$$

$$\chi_2=\exp\left\{\frac{1}{2}+\frac{16\pi^2}{6g^2}+\frac{1}{2}\left[\left(1+\frac{16\pi^2}{3g^2}\right)^2-\frac{64\pi^2}{\lambda}\frac{16\pi^2}{3g^2}\right]^{1/2}\right\}\mu^2. \tag{3.26}$$

In the limit that the gauge coupling becomes zero we have

$$\chi_1\underset{g^2\to0}{\sim}\exp\left(\frac{16\pi^2}{\lambda}\right)\mu^2,\qquad \chi_2\underset{g^2\to0}{\sim}\infty\,. \tag{3.27}$$

Then the orbit reduces to that of $\lambda\phi^4$ theory (Fig. 1) and we recover exactly the same results as that of Sec. II.

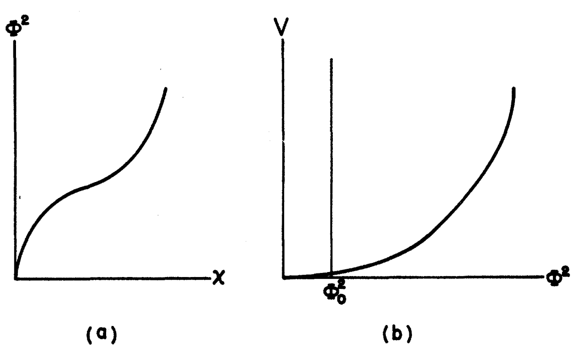

FIG. 8. Typical behavior of the orbit and the effective potential in phase I.

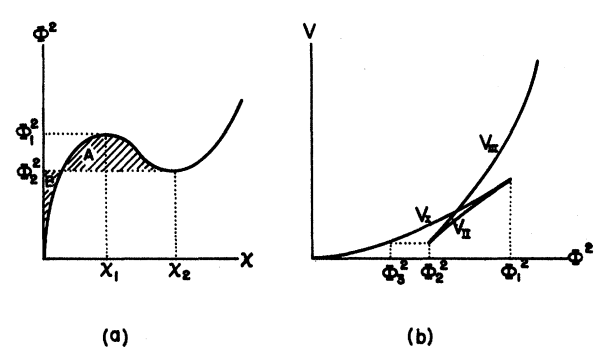

FIG. 9. Typical behavior of the orbit and the effective potential in phase II.

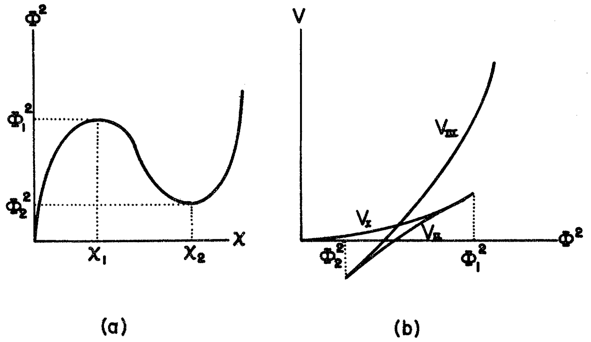

FIG. 10. Typical behavior of the orbit and the effective potential in phase III.

It is apparent from Figs. 9, 10, and 11 that the three phases are characterized by the value taken by ${\Phi_2}^2$,

phase II: ${\Phi_2}^2>0$ and $V({\Phi_2}^2)>0$,

phase III: ${\Phi_2}^2>0$ and $V({\Phi_2}^2)<0$,

phase IV: ${\Phi_2}^2<0$ and $V({\Phi_2}^2)<0$.

The boundary between phases II and III is to be obtained by the condition $V({\Phi_2}^2)=0$. Since $V(\Phi^2)$ can be calculated by quadratures as in Eq. (2.14), we have from Fig. 9 that

$$V({\Phi_2}^2)=B-A \tag{3.28}$$

and $A=B$ on the boundary. Therefore, we obtain the boundary between phases II and III by the *Maxwell construction*. The condition (3.28) can be explicitly calculated in terms of λ and g, and it becomes

$$\frac{16\pi^2}{\lambda}=\frac{1}{2}+\frac{1}{12}\,\frac{16\pi^2}{g^2}. \tag{3.29}$$

The other boundary divides the phases III and IV and ${\Phi_2}^2=0$ on it. This boundary can be readily obtained from Eqs. (3.23) and (3.26),

$$\frac{16\pi^2}{\lambda}=\frac{1}{2}+\frac{1}{12}\,\frac{16\pi^2}{g^2}-\frac{9}{4}\,\frac{g^2}{16\pi^2}. \tag{3.30}$$

The four phases divided by the boundaries (3.25), (3.29), and (3.30) are shown in Fig. 12.

A closer look at Figs. 8, 9, 10, and 11 reveals that the effective potential is real everywhere, although it could be multiple-valued. This is to be contrasted to the scalar field theory, where $V(\phi^2)$ becomes complex for large ϕ^2. The origin of the new feature is in the last term of Eq. (3.23). It is the dominant term for large Φ^2 and the plus sign of that term is crucial for the real effective potential.

We are now ready to study the ground state of the theory. We must look for the global minimum of $V(\Phi^2)$ for $\Phi^2 \geq {\Phi_0}^2$ with ${\Phi_0}^2$ given by (3.23). It is easy to observe that the effective potential attains its absolute minimum at $\Phi^2={\Phi_0}^2$ (or $\phi^2=0$) in phases I and IV. Therefore, the symmetry cannot be spontaneously broken in these phases. Furthermore, the scalar field theory which we have studied in Sec. II can be recovered by turning off the gauge coupling g; it belongs to phase IV. [We have already learned in Sec. II that the U(N)-symmetric $\lambda\phi^4$ theory does not break the symmetry spontaneously.]

However, symmetry breakdown can happen in phases II and III depending upon the value of ${\Phi_0}^2$. Since ${\Phi_0}^2$ is always positive in these phases (its proof is trivial), the symmetry is broken when

$${\Phi_3}^2<{\Phi_0}^2<{\Phi_2}^2 \text{ in phase II}$$

and

$$0<{\Phi_0}^2<{\Phi_2}^2 \text{ in phase III}.$$

This region of symmetry breakdown cannot be solved analytically in the λ-g^2 plane. Therefore, we have carried out numerical solutions for them, with the result shown in Fig. 12.

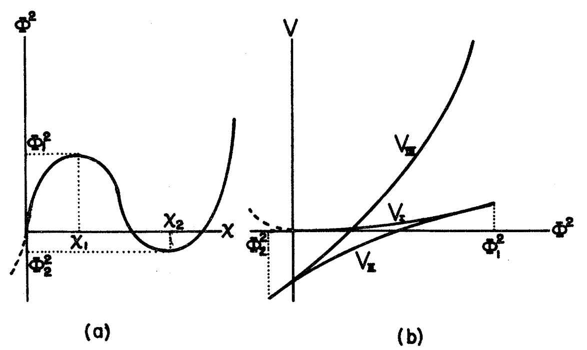

FIG. 11. Typical behavior of the orbit and the effective potential in phase IV.

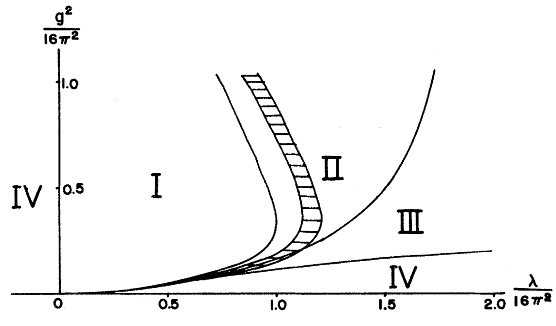

FIG. 12. Regions of various possible phases in the coupling-constant plane. The region of symmetry breaking is shown as a shaded area. Note that symmetry breaking is only possible in phases II and III.

It is interesting to observe that there is a narrow strip in the λ-g^2 plane where the symmetry is broken, no matter how small the gauge coupling might be.

Let us now fix the scalar coupling λ, and study the effective potential as a function of g^2. If λ is not too big, the theory goes through all the phases described above and the symmetry breaking can occur for large as well as small g^2. Recalling that we have calculated $V(\phi^2)$ to $O(g^2)$ in the gauge coupling, and to *all* orders in λ, we may rule out symmetry breaking for large g^2 as an artifact of the theory. However, symmetry breakdown for small g^2 is a reliable result of our theory, since the phenomenon exists for arbitrary small gauge coupling. The behavior of the effective potential is most clearly illustrated in Fig. 13 as a function of g^2.

F. Particle masses

In principle the particle masses are to be obtained from the pole structures of the Green's function, similar to the analysis of Eq. (2.18) in the scalar field theory. This is very complicated in the gauge theory which we are considering. There are two two-loop diagrams for the χ propagator and two one-loop diagrams for the scalar propagator in addition to the one shown in Fig. 3. However, the study could be greatly simplified if we are only interested in the leading terms of the masses and neglect $O(g^2)$ corrections. Then the scalar-boson masses are still given by Eq. (2.18), since any corrections due to the above-mentioned diagrams are of $O(g^2)$. The vector-boson masses are given by the tree approximation of the vector propagators.

When symmetry is not broken, N scalar bosons have degenerate mass $m_s{}^2$ which is simply the slope of the effective potential at the ground state,

$$m_s{}^2=\chi(0)\,. \tag{3.31}$$

Of course, the vector bosons are massless in this situation,

$$m_V{}^2=0\,. \tag{3.32}$$

However, in the event of symmetry breakdown an interesting thing happens very similar to the Higgs phenomenon, since $N-1$ transverse components of the scalar fields are absorbed by the gauge fields and accordingly $N-1$ gauge bosons become massive. The residual symmetry becomes U($N-1$). The mass of the remaining scalar boson is to be calculated from

$$D(\chi,\phi^2;-m_s{}^2)=0 \text{ with } \chi,\phi^2 \text{ at the ground state,} \tag{3.33}$$

where the D function is given by Eq. (2.20). It is

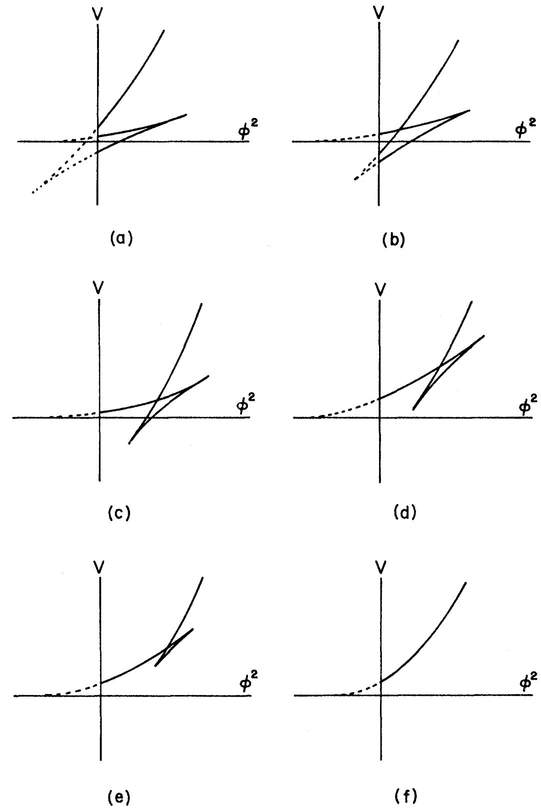

FIG. 13. Typical behavior of the effective potential as the gauge coupling is increased. The scalar coupling is fixed at $\lambda/16\pi^2<1$. $V(\phi^2)$ for $\phi^2<0$ is plotted as dotted lines to show the relationship with Figs. 8, 9, 10, and 11 and does not mean that it is complex there.

also evident from the tree approximation of the gauge boson propagators that the masses of the gauge bosons are

$$m_V{}^2=2g^2\phi^2 \text{ with } \phi^2 \text{ at the ground state.} \tag{3.34}$$

A typical behavior of the particle masses is plotted in Fig. 14 as a function of g^2 with λ fixed.

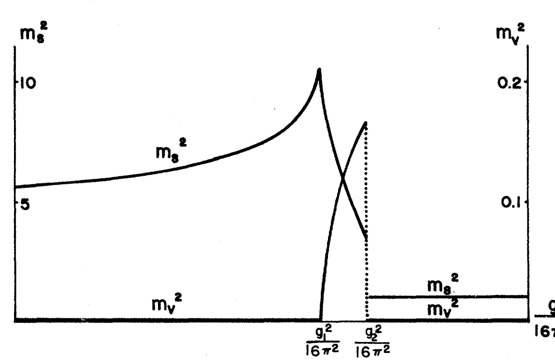

FIG. 14. Numerical solutions for the scalar-boson and the vector-boson masses as a function of g^2. The scalar coupling is fixed at $\lambda/16\pi^2=0.9$ and $\mu^2=1$.

Symmetry is not broken until the gauge coupling reaches a certain critical value g_1^2 and the vector bosons are massless. Then the vector bosons begin to acquire masses until another critical value g_2^2 is reached. Beyond the second critical value of the gauge coupling, symmetry is restored and the vector bosons become massless suddenly. This is a most surprising result of our analysis. Although the effective potential changes smoothly, the absolute minimum of $V(\phi^2)$ may shift abruptly, which we can confirm from Figs. 13(d) and 13(e). Therefore, there could be a sudden vacuum transition.

The scalar mass is also interesting. It increases until the first critical point g_1^2, but decreases afterwards and stays constant above g_2^2. Recalling that the renormalization conditions (2.6) and (2.7) are defined on solution I, we can understand constant scalar mass for $g^2 > g_2^2$. In this region the ground state lies on solution I [see Figs. 13(e) and 13(f)], and the mass given by Eq. (3.31) states that $m_S^2 = \mu^2$. It is also easy to understand the scalar mass in other regions. The slope of the effective potential keeps increasing as we follow the orbit from solution I to solution II [Figs. 9(a), 10(a), and 11(a)]. Therefore, the scalar bosons become heavier than the renormalization mass μ in the range $0 < g^2 < g_1^2$, and also the larger g^2 gives the heavier scalar particles. In the region of symmetry breakdown the argument becomes complicated since the mass should be calculated from Eq. (3.33). The value of ϕ^2 increases in this region while the change of the slope is rather small. Therefore, the solution for zero of the D function in Eq. (2.20) requires a smaller scalar mass for large ϕ^2.

IV. DISCUSSIONS

The ground state plays an important role in quantum field theory since all other one-particle states and bound states should be constructed from this ground state of the theory. Furthermore, the symmetry of the ground state is the symmetry of all particle states. It can be most conveniently studied by the effective-potential method. By looking for the global minimum of the effective potential we are able to find the ground state and see if any symmetry of the theory is spontaneously broken. On the other hand, the $1/N$ expansion is a systematic way of approximating the exact theory. This is particularly suitable for the study of the strong-coupling theory, since ordinary perturbation expansion is only valid in the weak-coupling limit. In this paper we have investigated the large-N limit of a gauge theory. Among our findings are the effective potential which is real everywhere, and a region of the coupling-constant space where symmetry is spontaneously broken.

The tachyon problem is not studied in this paper. It is much more complicated than the scalar field theory considered in Sec. II since two two-loop diagrams must be calculated for the χ propagator and the resulting propagator should be studied for *all* Euclidean momenta. However, we argue on the basis of the analysis in the scalar field theory that tachyons would not exist if we choose the global minimum of the effective potential. It is also to be noted that there are three complex solutions in addition to the real solutions of $V(\Phi^2)$ which we have discussed in Sec. III. They are the extrapolation of $V_I(\Phi^2)$ for $\Phi^2 < 0$, $V_I(\Phi^2)$ and $V_{II}(\Phi^2)$ for $\Phi^2 > \Phi_1^2$, and $V_{II}(\Phi^2)$ and $V_{III}(\Phi^2)$ for $\Phi^2 < \Phi_2^2$. Although the real part of the complex $V(\Phi^2)$ could be lower than $V_{II}(\Phi_2^2)$, we reject the possibility of choosing the ground state on the complex solutions for any ground state on the basis that the complex effective potential would be unstable and pose a tachyon problem. This is what has happened to the scalar field theory. The complex $V(\Phi^2)$ for $\Phi^2 > \Phi_1^2$ (see Fig. 2) goes to minus infinity for large Φ^2, and thus we can always find a vacuum state on the complex solution which is lower than $V_{II}(\Phi_0^2)$. However, it is easy to see from Eq. (2.20) that this vacuum state generates a tachyon, and should be rejected as an unphysical vacuum. Thus, we should restrict the discussion to the domain where $V(\Phi^2)$ is real.

Symmetry breakdown occurs for weak as well as strong gauge coupling. Any result associated with strong gauge coupling may be excluded from our consideration as an artifact of the theory, since we have approximated the $1/N$ expansion to the lowest order in g^2. Nevertheless the phenomenon of symmetry breaking for the weak gauge coupling region persists no matter how small the gauge coupling constant g^2 may be, and it is a genuine effect of the $1/N$ expansion. It is also to be noted from Fig. 12 that the scalar self-coupling is of the same order of magnitude as the gauge coupling when symmetry breakdown occurs,

$$\lambda = O(g^2). \tag{4.1}$$

Furthermore, in this region the mass ratio becomes

$$\frac{m_V^2}{m_S^2} = O(g^2). \tag{4.2}$$

The result may look unusual since Eq. (4.1) suggests that the mass ratio is of $O(1)$ if $m_S^2 = O(\lambda\phi^2)$ and $m_V^2 = O(g^2\phi^2)$. The part of the argument appropriate to the vector-boson mass is correctly given by Eq. (3.34), but the scalar-boson mass does not follow this naive argument. Instead, it must be calculated from Eq. (3.33). If the slope of the effective potential were zero at the ground state, then Eq. (2.20) would give $m_S^2 = O(\lambda\phi^2)$. However, the slope of $V(\phi^2)$ does not vanish at the minimum [see Figs. 13(c) and 13(d)]. Therefore, the scalar mass is of order unity.

Now we shall compare our result with other well-known symmetry-breaking schemes such as the Higgs phenomenon and symmetry breakdown of the Coleman-Weinberg type. These phenomena are discussed only in the context of the ordinary perturbation expansion, where *all* the coupling constants are small. We have shown in Eq. (3.27) that the effective potential with solution III, $V_{\rm III}$, becomes infinite in the weak-gauge-coupling limit. We have also argued at the end of Sec. II that $V_{\rm II}$ becomes minus infinity in the weak scalar coupling limit. Therefore, the ordinary perturbative effective potential corresponds to $V_{\rm I}$ in the weak-coupling limit, and the two schemes mentioned above are to be attributed to symmetry breakdown which results when the effective potential restricted to solution I develops a minimum. However, in our scheme symmetry is spontaneously broken as a result of higher-order quantum corrections which generates another solution of the effective potential $V_{\rm II}$, and gives a lower ground state than solution I. It is also interesting to note that the mass ratio in the Higgs scheme is

$$\frac{m_V^2}{m_S^2} = O(1) \tag{4.3}$$

since $\lambda = O(g^2)$ and $m_S^2 = O(\lambda\phi^2)$ in that scheme. In the Coleman-Weinberg type mechanism the scalar coupling λ is of $O(g^4)$, and the mass ratio becomes

$$\frac{m_V^2}{m_S^2} = O(1/g^2)\,. \tag{4.4}$$

Therefore, the $1/N$ expansion provides still another method of dynamical symmetry breaking, with the mass ratio m_V^2/m_S^2 of $O(g^2)$.

The $1/N$ expansion is a well-defined, systematic expansion method with N as its expansion parameter, just as in the same way the ordinary perturbation is characterized by a systematic expansion in the number of loops contained in the Feynman diagram. Since the $1/N$ expansion contains much more of the nonlinear structure of the complete theory than the ordinary perturbation expansion, we are able to explore a richer set of possibilities for symmetry breaking. Of course the well-known Higgs or Coleman-Weinberg mechanisms can be recovered in some particular weak-coupling limit of the $1/N$ expansion.

ACKNOWLEDGMENT

The author would like to thank Professor Howard J. Schnitzer for a critical reading of the manuscript and many illuminating discussions on this work.

---

*Research supported by ERDA under Contract No. E(11-1)3230.

[1]L. Dolan and R. Jackiw, Phys. Rev. D 9, 3320 (1974); H. J. Schnitzer, *ibid.* 10, 1800 (1974); 10, 2042 (1974); see also K. G. Wilson, *ibid.* 7, 2911 (1973).

[2]G. 't Hooft, Nucl. Phys. B72, 461 (1974). See also G. 't Hooft, 1975 Erice lectures (unpublished); G. P. Canning, Phys. Rev. D 12, 2505 (1975).

[3]S. Coleman, R. Jackiw, and H. D. Politzer, Phys. Rev. D 10, 2491 (1974).

[4]R. G. Root, Phys. Rev. D 10, 3322 (1974).

[5]M. Kobayashi and T. Kugo, Prog. Theor. Phys. 54, 1537 (1975); R. W. Haymaker, Phys. Rev. D 13, 968 (1976); L. F. Abbott, J. S. Kang, and H. J. Schnitzer, *ibid.* 13, 2212 (1976).

[6]D. Gross and A. Neveu, Phys. Rev. D 10, 3235 (1975).

[7]F. Englert and R. Brout, Phys. Rev. Lett. 13, 321 (1964); P. Higgs, Phys. Lett. 12, 132 (1964); G. Guralnik, C. Hagen, and T. Kibble, Phys. Rev. Lett. 13, 585 (1964); P. Higgs, Phys. Rev. 145, 1156 (1966); T. Kibble, *ibid.* 155, 1554 (1967).

[8]S. Coleman and E. Weinberg, Phys. Rev. D 7, 1888 (1973).

[9]Y. Nambu, Phys. Lett. 26B, 626 (1968); D. G. Boulware and L. S. Brown, Phys. Rev. 172, 1628 (1968); B. C. DeWitt, *Dynamical Theory of Groups and Fields* (Gordon and Breach, New York, 1965).

[10]G. 't Hooft and M. Veltman, Nucl. Phys. B44, 189 (1972); C. G. Bollini and J. J. Giamiagi, Nuovo Cimento 12B, 20 (1972); J. F. Ashmore, Lett. Nuovo Cimento 4, 289 (1972); Commun. Math. Phys. 29, 177 (1973); for review, see, for example, G. Leibbrandt, Rev. Mod. Phys. 47, 849 (1975).

[11]J. Goldstone, Nuovo Cimento 19, 154 (1961); J. Goldstone, A. Salam, and S. Weinberg, Phys. Rev. 127, 965 (1962).

[12]N. N. Khuri, Phys. Rev. D 12, 2298 (1975).

[13]J. S. Kang, Phys. Rev. D 11, 1563 (1975).

[14]Alternatively we may regard A_μ as a collection of gauge fields corresponding to two simple groups U(1) and SU(N), but coupled to the scalar field with the same gauge coupling.

[15]R. Jackiw, Phys. Rev. D 9, 1686 (1974); for alternative methods, see Ref. 8 and H. J. Schnitzer, Phys. Rev. D 10, 1800 (1974); 10, 2042 (1974).

[16]See, for example, S. Lefschetz, *Introduction to Topology* (Princeton Univ. Press, New Jersey, 1949), Chap. II.

[17]See, for example, J. S. Kang, Phys. Rev. D 10, 3455 (1974), Eq. (3.5).

[18]For the two-loop integrals in the dimensional integration method, see, for example, Appendix B of Ref. 17.

[19]J. S. Kang, Phys. Rev. D 13, 851 (1976).